Data-driven analysis of the beauty hadron production in pp collisions at the LHC with Bayesian unfolding

Xiaozhi Bai[a,b] **Guangsheng Li**[a,b] **Yifei Zhang,**[a,b,1] **Qingyi Situ**[b] **Xiaolong Chen**[a,b]

[a]*State Key Laboratory of Particle Detection and Electronics*

[b]*University of Science and Technology of China, Hefei 230026, China*

E-mail: xiaozhi.bai@cern.ch, ego2017@mail.ustc.edu.cn, ephy@ustc.edu.cn

ABSTRACT: Heavy flavour production in proton-proton (pp) collisions provides insights into the fundamental properties of Quantum Chromodynamics (QCD). Beauty hadron production measurements are widely performed through indirect approaches based on their inclusive decay modes. A Bayesian unfolding data-driven analysis of the ALICE and LHCb data was performed in this study, which recovers the full kinematic information of the beauty hadrons via different inclusive decay channels. The corresponding beauty hadron production cross sections obtained after the Bayesian unfolding are found to be consistent within their uncertainties. The weighted average open beauty production cross sections are presented as a function of the transverse momentum and rapidity in pp collisions at $\sqrt{s} = 5.02$ TeV and $\sqrt{s} = 13$ TeV, respectively. The p_{T}-integrated open beauty production $\mathrm{d}\sigma/\mathrm{d}y$ and the total $\mathrm{b}\overline{\mathrm{b}}$ cross section $\sigma_{\mathrm{b}\overline{\mathrm{b}}}$ are also reported. The precision of these results significantly improves upon worldwide measurements, providing valuable validation and constraints on mechanisms of heavy flavour production in pp collisions at the LHC energies.

---

[1]Corresponding author.

Contents

1 Introduction

The production of heavy flavour (charm and beauty) plays a crucial role in both pp and heavy-ion collisions. The study of heavy flavour production is important to understand the fundamental theory of Quantum Chromodynamics (QCD). The masses of the heavy quarks are significantly larger than the typical QCD energy scale, therefore, heavy quark production cross section in pp collisions can be evaluated by perturbative QCD (pQCD) calculations [1, 2]. Precise measurements of heavy-flavour hadron production cross section are important to validate pQCD theory in pp collisions. Furthermore, the masses of the heavy flavour quarks are much larger than the typical temperature of the quark-gluon plasma (QGP), which is suggested to be created in heavy-ion collisions [3, 4]. They are predominantly produced by hard partonic scattering processes in the early stage of the heavy-ion collisions and thus experience the full evolution of the system [5, 6]. Therefore, the heavy flavour production measurements in pp collisions are essential to test pQCD calculations and provide a reference for studying the nuclear medium effects and the properties of the QGP in heavy-ion collisions.

The calculation of heavy flavour production in pp collisions according to QCD can be factorized into several independent terms [7, 8]: i) The Parton Distribution Functions (PDFs), describing the probability of the quark or gluon to carry a given fraction of the momentum of the incoming protons [9, 10] provide crucial inputs for the calculations and need to be constrained by experimental measurements. ii) The hard scattering cross sections refer to the probability to produce a heavy quark pair via a specific process, such as a gluon-gluon interaction. These probabilities can be calculated by pQCD [7, 11]. iii) The produced heavy flavour partons fragment into particular hadrons according to the so-called Fragmentation Functions (FFs). The FFs are a typical non-perturbative process and need to be constrained by measurements [12]. Therefore, the calculation of heavy flavour hadron production cross sections involves both the perturbative and non-perturbative aspects of QCD. The heavy quark production cross section is not only critical for verifying the framework for QCD calculations but also provide inputs for its calculation [13].

Several experimental measurements of the heavy flavour production are carried out in pp collisions from $\sqrt{s}$ =0.2 to 13 TeV by the STAR, LHCb, CMS and ALICE collaborations [14–19]. The direct reconstruction of open beauty hadrons is challenged by the large combinatorial background and low specific hadronic decay branching ratios. An indirect approach, through inclusive decay modes is commonly employed in experimental measurements, which relies on the decay of open beauty hadrons to specific products and channels. Non-prompt components, originating from open beauty hadron decays, are frequently utilized in experimental measurements to assess beauty production [20, 21]. For example, commonly studied decay channels of open beauty hadrons include non-prompt D-mesons, J/ψ, as well as single electrons and muons from heavy flavour decays [20, 22–26]. Given the very different masses of the corresponding decay products and their distinct decay kinematics, the measured non-prompt components p_{T}-differential distributions are impacted by the decay process and can not directly reflect the beauty hadrons production. Consequently, different measured results are often discussed individually for specific decay channels, despite originating from the same underlying beauty production and merely representing different decay channels.

The Bayesian Unfolding has been employed since 1994, initially introduced by G. D'Agostini. It is a statistical technique used to recover the entire information based on the partial experimental data via the statistical approach, namely the semi-measurements [27]. This method is grounded in Bayesian statistical theory, which interprets probability as a measure of certainty, given prior theoretical inputs of the typically expected distribution [28, 29]. Bayesian unfolding offers a framework that explicitly incorporates uncertainties in both the measurements and the prior inputs. One of the key features is its ability to provide a systematic way of evaluating the uncertainties associated with the unfolding process itself, including both statistical and systematic uncertainties [27].

In this article, the systematic study of the total beauty production cross section is carried out through the data-driven analysis via Bayesian unfolding. The new results of the total beauty production cross section as a function of the p_{T}, rapidity y, and the centre-of-mass energy are reported. The unfolded results from different experimental measured decay channels, namely non-prompt D^0 at midrapidity ($|y| < 0.5$) and J/ψ at forward rapidity (2.0 $< y < 4.5$), are found to be perfectly compatible within their uncertainties. The weighted averaged results are computed with the weights evaluated according to the uncorrelated uncertainties of the considered inclusive decay modes mentioned above. The total b$\bar{\mathrm{b}}$ cross section is evaluated by integrating over p_{T} and y. The precision of this new approach is improved significantly compared with the previous ALICE published measurements via its individual decay channel.

The article is organized as follows: Section 2 provides the detailed description of the Bayesian unfolding statistical analysis method. A brief discussion of the uncertainties in this statistical analysis method is provided in Section 3. The results of the total beauty production cross sections obtained through the Bayesian unfolding method, along with comparisons to previously published results from various measurements and theoretical pQCD calculations are presented in Section 4. The discussions and conclusions from the results and the implications for the underlying physics are summarized in Section 5.

2 Bayesian unfolding statistical analysis method

Bayesian unfolding is a statistical analysis technique used to infer the entire distribution based on partial information. In this article, a data-driven approach is used to carry out the inclusive measurements of open beauty hadron production via non-prompt D^0 and J/ψ, i.e., the semi-inclusive decay of B^0, $B^\pm$, B_s^0, $\Lambda_b \to J/\psi$ +X and B^0, $B^\pm$, B_s^0, $\Lambda_b \to D^0$ +X [22, 30–32]. The decay products X are not used in the beauty hadron reconstruction. However, the missing information from the X component can be included in the simulation in the response matrix between the kinematic variables of the open beauty hadron and its decay products. Bayesian unfolding is a powerful technique for recovering the open beauty hadron entire information from its decay products. The essential idea is presented as follows in Eq. 2.1, the Bayes' theorem allows to invert the response from A to B to a response from B to A, the latter being better known than the former. The $P(A \mid B)$ is the probability of A given B, $P(B \mid A)$ is the probability of B given A, $P(A)$ is the prior probability of A, and $P(B)$ is the prior probability of B.

$$P(A \mid B) = \frac{P(B \mid A) \cdot P(A)}{P(B)} \qquad (2.1)$$

The concept of this approach can be elucidated by the Eq. 2.2, where $f_M(x)$ and $f_T(y)$ represent the measured non-prompt products and open beauty hadron distributions of the quantities x and y, respectively. The correspondence between quantities x and y is described by a response matrix $R(x|y)$, which transforms the original distribution $f_T(y)$ into the measured distribution $f_M(x)$.

$$f_M(x) = \int R(x|y) f_T(y) dy \qquad (2.2)$$

The realistic measured data are sorted into various bins such as p_T, y, or multiplicity intervals. The original (or expected) distributions are represented as $E_i(i = 1, 2, ...n)$. Subsequently, after accounting for the correspondence between measurements and expectations through unfolding techniques utilizing the transformation U_{ij}, Eq. 2.2 follows a summation form, as shown in Eq. 2.3. Consequently, constraints for each bin interval (E_i), and for a given effect like the open beauty hadron decay p_T smearing, can be generated from different bins $M_j(j = 1, 2, ...m)$ via migration. $P(M_j|E_i)$ can represent the efficiency of reconstruction, decay response, or any other unknown effects, but it should be understood through simulation.

$$E_i = \sum_{j=1}^{m} U_{ij} M_j \qquad (2.3)$$

$$U_{ij} = P(E_i|M_j)/\epsilon_i = P(M_j|E_i) \cdot P(E_i)/P(M_j)/\epsilon_i, \qquad (2.4)$$

$$\epsilon_i = \sum_{j=1}^{m} P(M_j|E_i) \qquad (2.5)$$

The expression for U_{ij} is explained by Eq. 2.4, and the details have been discussed in the previous equation 2.1. The response matrix delineates the correlation between measured data and the expected values of beauty hadrons. It is derived through EvtGen [33] simulations, EvtGen is a Monte Carlo event generator specifically designed for simulating the decays of heavy flavour hadrons, particularly beauty hadron decays. Additionally, the energy loss in the final state radiation is considered and simulated by the PHOTOS package [34]. All the detected efficiency including the decay acceptance, and decay branching ratio effects for observing non-prompt D^0 and non-prompt J/ψ, can be described by ϵ_i, which is defined in Eq. 2.5. The illustration of the response matrix of the beauty hadrons decays into D^0 and J/ψ are shown in pp collisions at $\sqrt{s} = 5.02$ TeV on the Fig. 1, in the left and right panels, respectively.
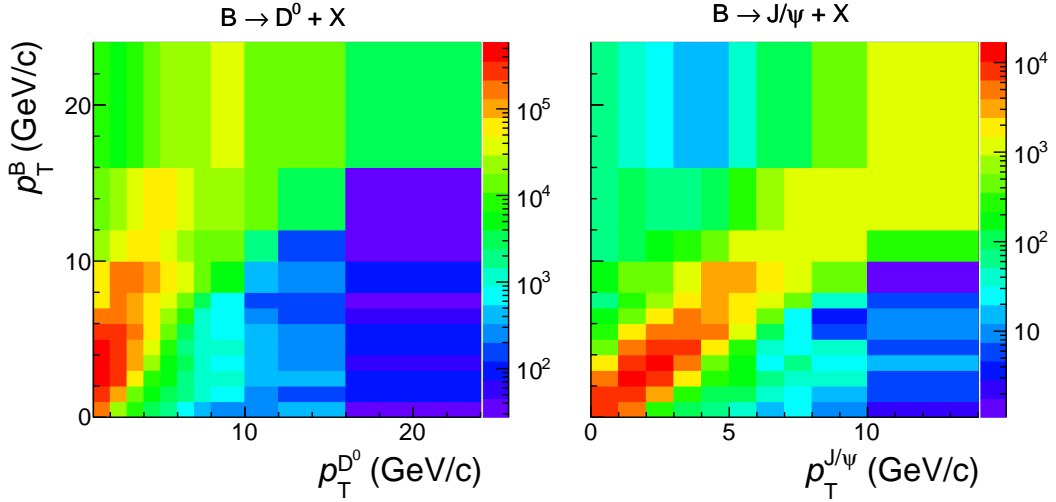

Figure 1. Response matrix of the beauty hadrons as a function of the non-prompt D^0 (left panel) and J/ψ (right panel) in pp collisions at $\sqrt{s} = 5.02$ TeV at rapidity interval $|y| < 10$.

Equation 2.3 and 2.4 need the knowledge of the beauty hadron original distribution E_i, which is not known, so it is necessary to start from a prior distribution from FONLL calculations and then though the iterative method to have a better estimation of it, as described in Ref. [35]. Uncertainties are evaluated and systematically propagated, with the cumulative effect of all iterations taken into account. The iteration is halted once the difference between the current and previous iterations is significantly smaller than the uncertainties.

3 Uncertainties analysis

The sources of uncertainty considered in this study are dominated by the uncertainties of the measured non-prompt D^0 and non-prompt J/ψ, as well as semi-inclusive beauty hadrons (B^0, $B^\pm$, B_s^0, Λ_b) decay branching ratio to D^0 and J/ψ. Furthermore, the statistical uncertainties of the unfolding matrix, the number of Bayesian iterations, and the

extrapolation of non-prompt D^0 p_T down to 0 are considered as the remaining systematical uncertainties. The evaluated total uncertainties are summarized in Table 1, details are discussed in this section.

The main uncertainties originate from the measured data of non-prompt D^0 and J/ψ [22, 30–32]. The non-prompt D^0 results provided by ALICE introduce relatively larger uncertainties compared to J/ψ, the latter measured by LHCb. The statistics and systematical uncertainties of measured non-prompt D^0 and J/ψ, are propagated separately to the final open beauty hadron production cross section. The statistical uncertainties can be considered independent over p_T, while the systematic uncertainties should be partially correlated among different p_T bins. The extent of this correlation is not straightforward to be determined. Therefore, two extreme assumptions are validated: fully correlated and independent. These correspond to the values of 4.3% and 2.3% for $\sqrt{s} = 5.02$ TeV, and 5.2% and 2.8% for $\sqrt{s} = 13$ TeV, respectively. The fully correlated case is considered by default, and results are reported in Table 1. Therefore, the systematic uncertainties from the measured non-prompt D^0 and J/ψ are conservatively overestimated in this study.

The uncertainties of the inclusive beauty hadron decay to D^0 and J/ψ, are considered as global uncertainty, they are provided by the Particle Data Group (PDG). The statistical uncertainty of the response matrix in the unfolding process can be reduced by increasing the statistics of the EvtGen simulation, and it is below 1% in this study. The uncertainty of the number of Bayesian iterations is evaluated by comparing the results of iterations 4 and 6, and the difference between the two cases is found to be much smaller than the statistical uncertainties. The discrepancy between the former and later iterations is around 1%, which is considered as the systematical uncertainty of the number of iterations.

The minimum p_T of the measured non-prompt D^0 by ALICE is 1 GeV/c, while the measured non-prompt J/ψ by LHCb extends down to 0 GeV/c. Ideally, no extrapolation is needed of the p_T, as the contribution of unmeasured p_T and y intervals should be recovered by the unfolding process. The difference in results with and without the extrapolation is lower than 1%. The difference between with and without extrapolation is considered as the uncertainty of the measured non-prompt D^0 p_T down to 0.

The uncertainty on the beauty hadron p_T shape for the realistic response matrix creation is considered as the last component of the systematical uncertainties. This is evaluated via re-weighting the p_T shape of the open beauty hadron used for the response matrix creation, using two different p_T shapes: one from PYTHIA and another from the FONLL prediction. The corresponding discrepancy observed on the final results is around 1% for all cases, except for non-prompt J/ψ at $\sqrt{s} = 13$ TeV, where it is 5.2%.

Different sources of uncertainties are described, the correlated and uncorrelated uncertainties are evaluated and propagated separately, and the corresponding values are listed in Table 1. The final uncertainties are summed up in quadrature. The weighted average total uncertainties for $b\bar{b}$ production cross section at midrapidity are 8.2% and 8.1% for $\sqrt{s} = 5.02$ TeV and $\sqrt{s} = 13$ TeV, respectively.

Table 1. Systematic uncertainties on the p_T-integrated $b\bar{b}$ cross section, obtained from the Bayesian unfolding in pp collisions at $\sqrt{s}$ = 5.02 and $\sqrt{s}$ = 13 TeV at midrapidity, are reported. The individual contributions and the total uncertainties are given in percentage. It is considered that all the systematical uncertainties are correlated over p_T.

Uncertainty sources	$\sqrt{s}$ = 5.02 TeV			$\sqrt{s}$ = 13 TeV		
	D^0	J/ψ	average	D^0	J/ψ	average
Measured non-prompt data stat.	9.1	0.4	2.6	4.2	0.5	2.1
Measured non-prompt data syst.	10.5	4.4	4.3	8.4	6.2	5.2
Response matrix stat.	< 0.1	0.7	0.5	< 0.1	0.3	0.1
Branching ratio of h_B decay	5.8	8.6	6.4	5.8	8.6	5.2
Bayes iterations	0.3	1.4	1.0	0.6	< 0.1	0.3
W/o p_T extrapolation	0.1	N/A	< 0.1	0.4	N/A	0.2
Beauty hadron p_T shape	1.0	0.8	0.6	1.6	5.2	2.7
Total uncertainty	15.2	9.8	8.2	11.2	11.8	8.1

4 Results

In this section, p_T-differential ($d\sigma/dp_T$) as well as y-differential ($d\sigma/dy$, p_T >0) cross section results of $b\bar{b}$ production are provided in pp collisions at $\sqrt{s}$ = 5.02 and 13 TeV. These results are obtained from the Bayesian unfolding procedure applied to the measured non-prompt D^0 and non-prompt J/ψ cross section measurements at the same energies. The unfolded results are corrected by the inclusive beauty hadrons (B^0, $B^\pm$, B_s^0, Λ_b) decay to J/ψ and D^0 branching ratio from PDG, the values are $60.4 \pm 3.5\%$ and $1.16 \pm 0.10\%$ for D^0 and J/ψ, respectively.

The critical inputs of unfolding analysis are the measured non-prompt components from the open beauty hadron decays. The measured non-prompt D^0 from ALICE [30] and non-prompt J/ψ [31] from LHCb are used in pp collisions at $\sqrt{s}$ = 5.02 TeV analysis, while the similar inputs in pp collisions at $\sqrt{s}$ = 13 TeV can be found in Refs. [22, 32]. The p_T-differential production cross section $d\sigma/dp_T$ via Bayesian unfolding analysis is shown at rapidity interval |y| < 10 in Fig. 2. The data points represent the results obtained by unfolding from the two aforementioned inclusive decay channel measurements of non-prompt D^0 (red) and non-prompt J/ψ (blue). The results of $b\bar{b}$ production cross section $d\sigma/dp_T$ as a function of the p_T in pp collision at $\sqrt{s}$ = 5.02 TeV and $\sqrt{s}$ = 13 TeV are shown in the left and right panels, respectively. The results derived from two different semi-inclusive decay channels (non-prompt D^0 and non-prompt J/ψ) are compared in the two upper panels, and the corresponding ratios are shown in two lower panels. It is found that different semi-inclusive decay channels are perfectly consistent within their uncertainties after unfolding the beauty hadron to the same rapidity intervals (|y| < 10), although the measured non-prompt D^0 and non-prompt J/ψ are from very different rapidity coverage. The non-prompt D^0 is measured at midrapidity (|y| < 0.5), while the non-prompt J/ψ measurements are at forward rapidity (2.5 < y < 4), the large rapidity gap is recovered by the unfolding matrix. This is expected, as they originate from the decay of the same underlying beauty hadrons once they are unfolded to identical kinematic ranges. The

consistency indicates the unfolding matrix produced by the EvtGen describes properly the dependence of open beauty hadron and its decay products. Small differences among different decay channels could result from statistical fluctuations in the measured non-prompt D^0 and J/ψ. Furthermore, the consistences can provide an important cross check among the measurements provided by different collaborations.
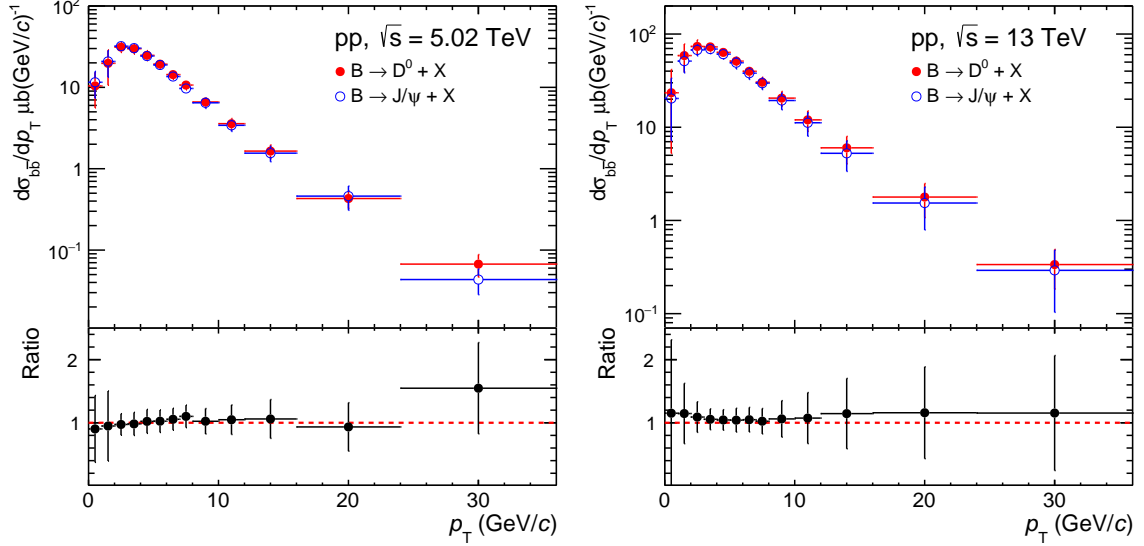

Figure 2. The $b\bar{b}$ production cross section $d\sigma/dp_T$ as a function of p_T in pp collisions at $\sqrt{s} = 5.02$ TeV (left panel) and $\sqrt{s} = 13$ TeV (right panel) at rapidity interval $|y| < 10$, the data points represent the unfolded results from the decay channels to non-prompt D^0 (red) and J/ψ (blue).

It is natural to compute the weighted average p_T-differential $b\bar{b}$ production cross section on results obtained from different decay channels, according to the Eq. 4.1. The inversed quadratic uncertainties are used as the weight factor in the computation of the averaged p_T-differential beauty hadron production cross sections, as shown in Eq. 4.2. This method has been utilized by ALICE for computing the averaged charm mesons production yields in Pb–Pb collision at $\sqrt{s_{NN}} = 5.02$ TeV [36]. The main idea behind this method is that data points with smaller uncertainties carry a relatively larger weight factor in combined results calculations.

$$d\sigma/dp_T(\text{ave.}) = \sum_{i=(D^0, J/\psi)} w(i) d\sigma/dp_T(i) \tag{4.1}$$

$$w(i) = \frac{1/\sigma_i^2}{\sum_{i=(D^0, J/\psi)} 1/\sigma_i^2} \tag{4.2}$$

The p_T-integrated $b\bar{b}$ production cross section per unit of rapidity $d\sigma/dy$ in pp collisions at $\sqrt{s} = 5.02$ TeV, is calculated by the integral of the weighted average p_T-differential cross section $d\sigma/dp_T$. The p_T-integrated uncertainties need to consider the correlation over p_T. The bin immigration is simulated by the unfolding, and the correlations between
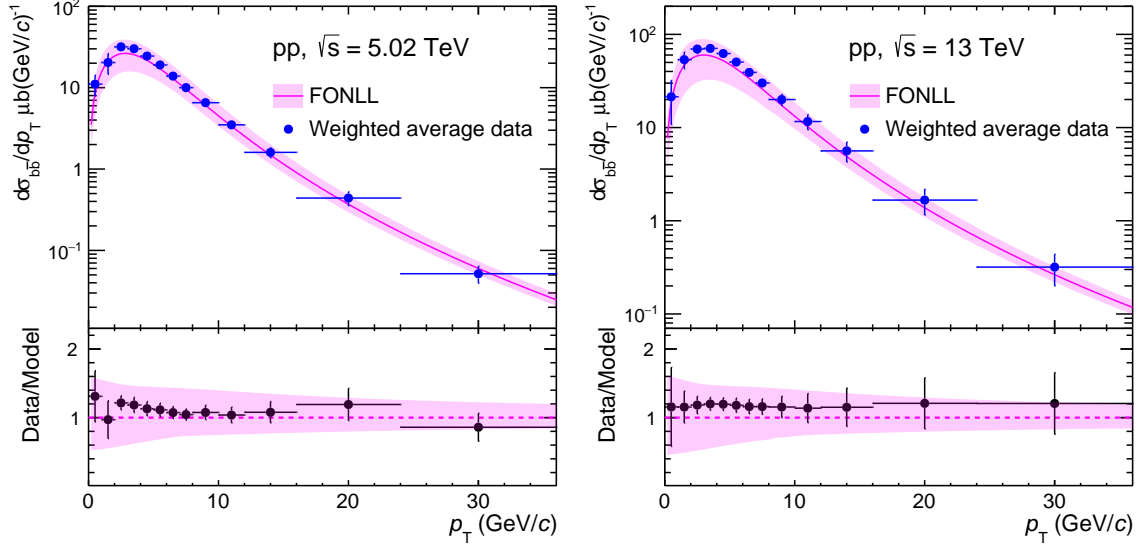
Figure 3. The comparison of the weight averaged b$\overline{\text{b}}$ production cross section and the FONLL calculations as a function of p_{T} in pp collisions at $\sqrt{s}$ = 5.02 TeV (left panel)and $\sqrt{s}$ = 13 TeV (right panel), the ratios of the b$\overline{\text{b}}$ production cross section to FONLL calculations are shown in the two lower panels.

different bins are described by the covariance matrix, which is provided alongside with the unfolding matrix.

The results of the total b$\overline{\text{b}}$ cross section as a function of the rapidity in pp collisions at $\sqrt{s}$ = 5.02 TeV are shown in Fig. 4 left panel. The p_{T}-integrated b$\overline{\text{b}}$ production cross section is compared with the FONLL predictions. The FONLL calculation can describe the unfolded results within the rapidity interval |y| < 4.5, despite its large uncertainties in the calculations. To validate the FONLL calculations, the uncertainties of the calculation need to be improved. It is dominated by the PDFs for the low-p_{T} and large-y regions, and renormalisation and factorisation scales dominate the high-p_{T} and small-y regions.

The p_{T}-integrated b$\overline{\text{b}}$ production cross section per unit of rapidity dσ/dy in pp collisions at $\sqrt{s}$ = 13 TeV is obtained using the same procedures as in pp collisions at $\sqrt{s}$ = 5.02 TeV, the results are shown in Fig. 4 right panel. The agreement between data and FONLL calculation is slightly better at $\sqrt{s}$ = 5.02 TeV than at $\sqrt{s}$ = 13 TeV. The production cross section of b$\overline{\text{b}}$ pairs per unit of rapidity at midrapidity (|y| < 4.5) is evaluated independently for the non-prompt D^0 and J/ψ. It is not needed to apply p_{T} extrapolation procedures to extend the p_{T} coverage down to 0 for the ALICE measured D^0. The absence of low p_{T} cross sections of the non-prompt unmeasured D^0 is corrected by unfolding procedures, while the non-prompt J/ψ is measured down to p_{T} = 0. Eventually, the b$\overline{\text{b}}$ pair production cross sections are evaluated from 0 and to 36 GeV/c, and the contribution from p_{T} greater than 36 GeV/c is much less than 1%, which is negligible to the total b$\overline{\text{b}}$ cross section. The results from two channels are combined as a weighted average according to their uncertainties, as two measurements are provided by two collaborations. The uncertainties can be considered
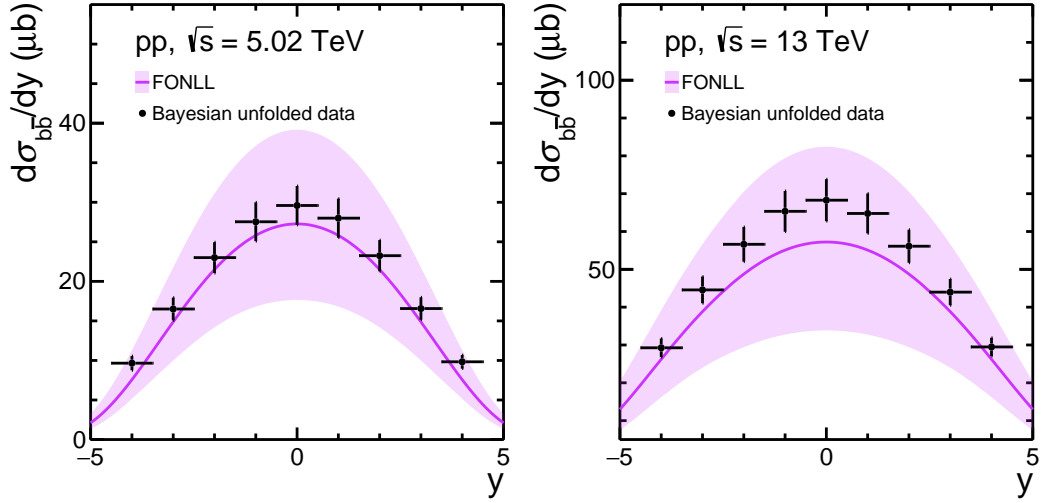
Figure 4. The comparison of the weighted average p_{T}-integrated $b\bar{b}$ production cross section and the FONLL calculations as a function of rapidity(y) in pp collisions at $\sqrt{s} = 5.02$ TeV (left panel) and $\sqrt{s} = 13$ TeV (right panel).

independent, so the total uncertainties are used in the weight factor calculation, as shown by Eq. 4.1 and 4.2.

The total $b\bar{b}$ production cross section at midrapidity is obtained in pp collision at $\sqrt{s}$ = 5.02 TeV and $\sqrt{s}$ = 13 TeV. The correlated and uncorrelated uncertainties are propagated accordingly, following the same procedure as $d\sigma/dy$ calculation described previously in this section. The final results of the total $b\bar{b}$ production cross section at midrapidity are presented in Fig. 5 for $\sqrt{s}$ = 5.02 TeV and $\sqrt{s}$ = 13 TeV. The new results are compared with the worldwide results provided by ALICE [30, 37–39]. Furthermore, the new results are compared to the FONLL predictions, which are shown both for $\sqrt{s}$ = 5.02 TeV and $\sqrt{s}$ = 13 TeV. The new $b\bar{b}$ cross section at midrapidity from the unfolding is compatible with the reported worldwide results by ALICE, as well as with PYTHIA and POWHEG. The uncertainties have been significantly improved compared to the worldwide presented results. The new results also agree with the FONLL predictions within their large uncertainties. The new $b\bar{b}$ production cross section can be expected to provide constraints on the FONLL calculations, helping to further reduce the corresponding uncertainties of the FONLL predictions.

The total $b\bar{b}$ cross section at midrapidity in pp collisions at $\sqrt{s}$ = 5.02 TeV and $\sqrt{s}$ = 13 TeV are shown as a function of centre-of-mass energy in Fig. 6, together with other experimental measurements in pp collisions from 1.96 up to 13 TeV. The results are provided by ALICE [30, 37, 40, 41] and similar results in p$\bar{\mathrm{p}}$ collisions from CDF [42]. The measured results from dielectron by ALICE collaboration [38, 39, 43], either PYTHIA or POWHEG simulations, are added as well for comparison. The FONLL calculations can describe the data within its large uncertainties, despite the experimental points sitting on the upper side of the FONLL calculations. The $b\bar{b}$ production cross section $d\sigma/dy$ at midrapidity
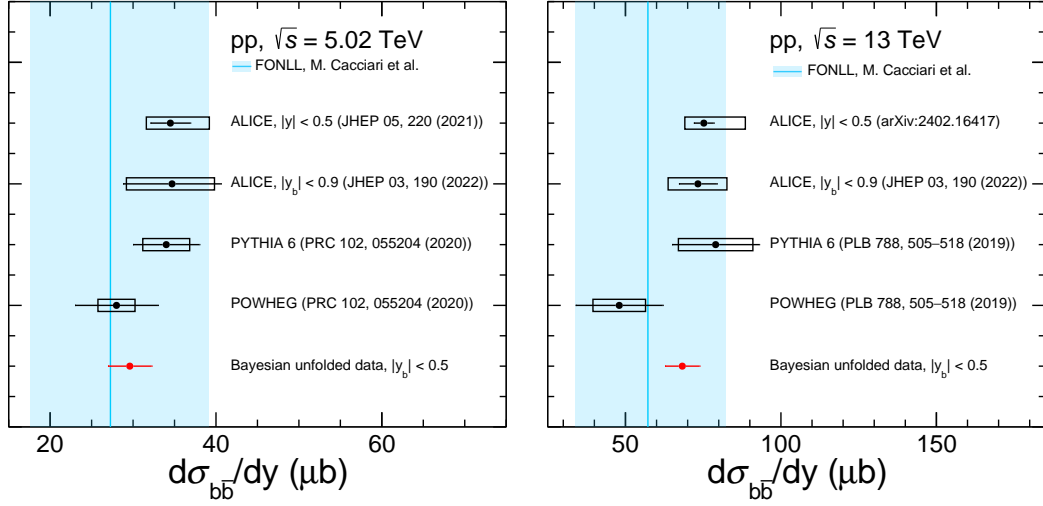
Figure 5. Weight average b$\bar{\text{b}}$ production cross section in pp collisions at $\sqrt{s}$ = 5.02 TeV (left) and $\sqrt{s}$ = 13 TeV (right) at midrapidty, the results are compared with the existing measurements from ALICE collaboration [22, 30, 37–39] and FONLL predictions.

are:

$$\frac{\mathrm{d}\sigma_{\mathrm{b\bar{b}}}}{\mathrm{d}y}\Big|_{|y_{\mathrm{b}}|<0.5}^{\sqrt{s}=5.02\mathrm{TeV}} = 29.6 \pm 2.4 \ \mu\mathrm{b},$$

$$\frac{\mathrm{d}\sigma_{\mathrm{b\bar{b}}}}{\mathrm{d}y}\Big|_{|y_{\mathrm{b}}|<0.5}^{\sqrt{s}=13\mathrm{TeV}} = 68.3 \pm 5.5 \ \mu\mathrm{b}$$

in pp collisions at $\sqrt{s}$ = 5.02 TeV and $\sqrt{s}$ = 13 TeV, respectively. The uncertainties, including the statistical and systematical uncertainties from the measured non-prompt D^0 and J/ψ, are propagated separately. The statistical uncertainties are considered independent over p_{T}, while the systematic uncertainties including the global uncertainty are considered fully correlated over p_{T}. This extreme assumption overestimates the measured non-prompt systematical uncertainties. Further discussion on the total uncertainties can be found in the previous section 3.

The total b$\bar{\text{b}}$ production cross section $\sigma_{\mathrm{b\bar{b}}}$ in the full phase space in pp collisions at $\sqrt{s}$ = 5.02 TeV and $\sqrt{s}$ = 13 TeV are:

$$\sigma_{\mathrm{b\bar{b}}}^{\sqrt{s}=5.02\mathrm{TeV}} = 191.3 \pm 16.2 \ \mu\mathrm{b},$$

$$\sigma_{\mathrm{b\bar{b}}}^{\sqrt{s}=13\mathrm{TeV}} = 499.8 \pm 39.6 \ \mu\mathrm{b}$$

The full phase space 4π is simulated by the unfolding matrix without any y or p_{T} extrapolation. The propagation procedures of the uncertainties are the same as those for the b$\bar{\text{b}}$ cross section at midrapidity $\mathrm{d}\sigma/\mathrm{d}y$ evaluations. The new results of the total beauty production cross section in 4π full phase space are found to be consistent with the combined results of the LHCb and ALICE non-prompt J/ψ via the extrapolation approach [37], where
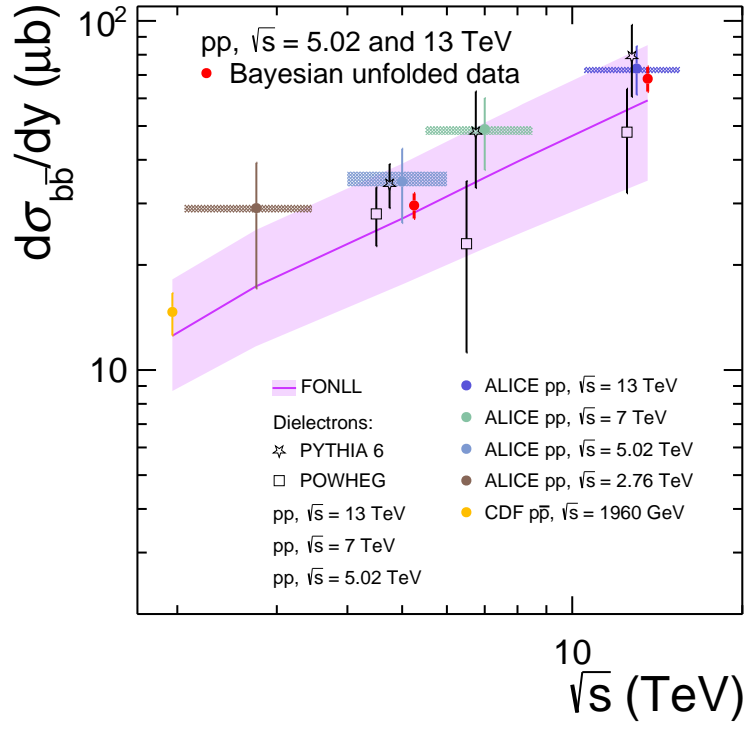
Figure 6. Total b$\bar{\text{b}}$ production cross section as a function of centre-of-mass energies at midrapidity in pp collisions, the results are compared with the worldwide measurements [30, 37–43] and the FONLL calculations.

the full phase space extrapolations factor $\alpha_{4\pi}$ is extracted from the FONLL calculations.

5 Conclusions

The b$\bar{\text{b}}$ production cross sections in pp collisions at centre-of-mass energy at $\sqrt{s} = 5.02$ TeV and $\sqrt{s} = 13$ TeV are obtained by using the Bayesian unfolding based on the measured non-prompt D^0 and non-prompt J/ψ mesons. The new results are compared with the FONLL predictions, as well as with existing experimental measurements.

The Bayesian unfolded open heavy hadron and b$\bar{\text{b}}$ p_{T}-differential and integrated result obtained only from the ALICE non-prompt D^0 and only from the LHCb non-prompt J/ψ combined with the rapidity and p_{T}-shapes lead to mutually consistent results. Hence, this consistency provides critical cross-checks between different decay channels and measurement techniques. The weighted average results are computed according to the individual uncorrelated uncertainties. The FONLL prediction is in good agreement with Bayesian unfolding results within uncertainties in general, but the data is on the upper side of the FONLL calculation.

The p_{T}-integrated b$\bar{\text{b}}$ production cross sections dσ/dy in pp collisions are presented at $\sqrt{s} = 5.02$ TeV and $\sqrt{s} = 13$ TeV. The cross section is significantly higher at midrapidity than at forward rapidity. The FONLL predictions are consistent within uncertainties to the unfolded data. The total b$\bar{\text{b}}$ production cross section in the full phase space is compared with the existing data from ALCIE measurements from the individual non-prompt D^0 and non-prompt J/ψ measurements at the midrapidity, which was evaluated by extrapolating p_{T} down to 0, and the large uncertainties are introduced by extrapolating process.

The precision of the new results significantly improves the existing worldwide b$\bar{\text{b}}$ production cross section. This will provide valuable validation and trigger improvements in pQCD-based calculations in pp collisions in pp collisions. In addition, as the b$\bar{\text{b}}$ production cross sections scaling with the number of the binary collisions, and can be used as critical inputs for models of open beauty mesons, and baryons, as well as bottomonium-related calculations in heavy-ion collisions [44, 45]. Furthermore, these results can also serve as a good reference for future studies in heavy-ion physics. Finally, this study provides a show case for the usage of Bayesian unfolding relying on only partially reconstructed data from different experiments. The results are highly encouraging to employ the methodology to similar problems as the extraction of total c$\bar{\text{c}}$ and b$\bar{\text{b}}$ cross sections also in proton-nucleus, nucleus-nucleus and proton-proton collisions at different collision energies

References

[1] M. Cacciari, P. Nason, and R. Vogt, "QCD predictions for charm and bottom production at RHIC", *Phys. Rev. Lett.* **95** (2005) 122001, `arXiv:hep-ph/0502203`.

[2] S. Frixione, "Heavy flavors in perturbative QCD", *Eur. Phys. J. C* **43** (2005) 103–111.

[3] S. Catani, S. Devoto, M. Grazzini, S. Kallweit, and J. Mazzitelli, "Bottom-quark production at hadron colliders: fully differential predictions in NNLO QCD", *JHEP* **03** (2021) 029, `arXiv:2010.11906 [hep-ph]`.

[4] G. Kramer and H. Spiesberger, "Study of heavy meson production in p–Pb collisions at $\sqrt{S}$= 5.02 TeV in the general-mass variable-flavour-number scheme", *Nucl. Phys. B* **925** (2017) 415–430, `arXiv:1703.04754 [hep-ph]`.

[5] **ALICE** Collaboration, S. Acharya *et al.*, "Production of Muons from Heavy Flavor Decays at Forward Rapidity in *pp* and Pb-Pb Collisions at $\sqrt{s_{NN}}$=2.76 TeV", *JHEP* **09** (2019) 008, `arXiv:1905.07207 [nucl-ex]`.

[6] **ALICE** Collaboration, S. Acharya *et al.*, "Measurement of electrons from semileptonic heavy-flavour hadron decays at midrapidity in pp and Pb-Pb collisions at $\sqrt{s_{\mathrm{NN}}} = 5.02$ TeV", *Phys. Lett. B* **804** (2020) 135377, `arXiv:1910.09110 [nucl-ex]`.

[7] M. Cacciari, S. Frixione, N. Houdeau, M. L. Mangano, P. Nason, and G. Ridolfi, "Theoretical predictions for charm and bottom production at the LHC", *JHEP* **10** (2012) 137, `arXiv:1205.6344 [hep-ph]`.

[8] R. Maciula and A. Szczurek, "Open charm production at the LHC - k_t-factorization approach", *Phys. Rev. D* **87** no. 9, (2013) 094022, `arXiv:1301.3033 [hep-ph]`.

[9] H.-L. Lai, M. Guzzi, J. Huston, Z. Li, P. M. Nadolsky, J. Pumplin, and C.-P. Yuan, "New parton distributions for collider physics", *Phys. Rev. D* **82** (2010) 074024, `arXiv:1007.2241 [hep-ph]`.

[10] **NNPDF** Collaboration, R. D. Ball *et al.*, "Parton distributions from high-precision collider data", *Eur. Phys. J. C* **77** no. 10, (2017) 663, `arXiv:1706.00428 [hep-ph]`.

[11] J. Mazzitelli, A. Ratti, M. Wiesemann, and G. Zanderighi, "B-hadron production at the LHC from bottom-quark pair production at NNLO+PS", *Phys. Lett. B* **843** (2023) 137991, `arXiv:2302.01645 [hep-ph]`.

[12] A. Metz and A. Vossen, "Parton Fragmentation Functions", *Prog. Part. Nucl. Phys.* **91** (2016) 136–202, `arXiv:1607.02521 [hep-ex]`.

[13] M. Cacciari, M. Greco, and P. Nason, "The p_T spectrum in heavy-flavour hadroproduction.", *JHEP* **05** (1998) 007, `arXiv:hep-ph/9803400`.

[14] **STAR** Collaboration, M. S. Abdallah *et al.*, "Evidence of Mass Ordering of Charm and Bottom Quark Energy Loss in Au+Au Collisions at RHIC", *Eur. Phys. J. C* **82** no. 12, (2022) 1150, `arXiv:2111.14615 [nucl-ex]`. [Erratum: Eur.Phys.J.C 83, 455 (2023)].

[15] **LHCb** Collaboration, R. Aaij *et al.*, "Measurement of B meson production cross-sections in proton-proton collisions at $\sqrt{s} = 7$ TeV", *JHEP* **08** (2013) 117, `arXiv:1306.3663 [hep-ex]`.

[16] **LHCb** Collaboration, R. Aaij *et al.*, "Study of the production of Λ_b^0 and $\overline{B}^0$ hadrons in *pp* collisions and first measurement of the $\Lambda_b^0 \to J/\psi p K^-$ branching fraction", *Chin. Phys. C* **40** no. 1, (2016) 011001, `arXiv:1509.00292 [hep-ex]`.

[17] **LHCb** Collaboration, R. Aaij *et al.*, "Measurement of the *b*-quark production cross-section in 7 and 13 TeV *pp* collisions", *Phys. Rev. Lett.* **118** no. 5, (2017) 052002, arXiv:1612.05140 [hep-ex]. [Erratum: Phys.Rev.Lett. 119, 169901 (2017)].

[18] **CMS** Collaboration, V. Khachatryan *et al.*, "Measurement of the total and differential inclusive B^+ hadron cross sections in pp collisions at $\sqrt{s} = 13$ TeV", *Phys. Lett. B* **771** (2017) 435–456, arXiv:1609.00873 [hep-ex].

[19] **ALICE** Collaboration, S. Acharya *et al.*, "Measurement of D-meson production at mid-rapidity in pp collisions at $\sqrt{s} = 7$ TeV", *Eur. Phys. J. C* **77** no. 8, (2017) 550, arXiv:1702.00766 [hep-ex].

[20] **ALICE** Collaboration, S. Acharya *et al.*, "Prompt and non-prompt J/ψ production at midrapidity in Pb–Pb collisions at $\sqrt{s_{\mathrm{NN}}} = 5.02$ TeV", *JHEP* **02** (2024) 066, arXiv:2308.16125 [nucl-ex].

[21] **ALICE** Collaboration, S. Acharya *et al.*, "Measurement of beauty production via non-prompt D^0 mesons in Pb-Pb collisions at $\sqrt{s_{\mathrm{NN}}} = 5.02$ TeV", *JHEP* **12** (2022) 126, arXiv:2202.00815 [nucl-ex].

[22] **ALICE** Collaboration, S. Acharya *et al.*, "Measurement of beauty-quark production in pp collisions at $\sqrt{s} = 13$ TeV via non-prompt D mesons", arXiv:2402.16417 [hep-ex].

[23] **ALICE** Collaboration, S. Acharya *et al.*, "Measurement of electrons from beauty-hadron decays in pp and Pb-Pb collisions at $\sqrt{s_{\mathrm{NN}}} = 5.02$ TeV", *Phys. Rev. C* **108** no. 3, (2023) 034906, arXiv:2211.13985 [nucl-ex].

[24] **ATLAS** Collaboration, G. Aad *et al.*, "Measurement of azimuthal anisotropy of muons from charm and bottom hadrons in *pp* collisions at $\sqrt{s} = 13$ TeV with the ATLAS detector", *Phys. Rev. Lett.* **124** no. 8, (2020) 082301, arXiv:1909.01650 [nucl-ex].

[25] F. Si, X.-L. Chen, L. Zhou, Y.-F. Zhang, S.-H. Zhang, X.-Y. Ju, X.-J. Li, X. Dong, and N. Xu, "Charm and beauty isolation from heavy flavor decay electrons in Au+Au collisions at $\sqrt{s_{NN}} = 200$ GeV at RHIC", *Phys. Lett. B* **805** (2020) 135465, arXiv:1906.08974 [nucl-ex].

[26] D. Li, F. Si, Y. Zhao, P. Zhou, Y. Zhang, X. Li, and C. Yang, "Charm and beauty isolation from heavy flavor decay electrons in pp and Pb–Pb collisions at $\sqrt{s_{\mathrm{NN}}} = 5.02$ TeV at LHC", *Phys. Lett. B* **832** (2022) 137249, arXiv:2110.08769 [nucl-ex].

[27] G. D'Agostini, "Improved iterative Bayesian unfolding", *arXiv e-prints* (Oct., 2010) arXiv:1010.0632, arXiv:1010.0632 [physics.data-an].

[28] G. D'Agostini, "Asymmetric Uncertainties: Sources, Treatment and Potential Dangers", *arXiv e-prints* (Mar., 2004) physics/0403086, arXiv:physics/0403086 [physics.data-an].

[29] G. D'Agostini, "Bayesian inference in processing experimental data: principles and basic applications", *Reports on Progress in Physics* **66** no. 9, (Sept., 2003) 1383–1419, arXiv:physics/0304102 [physics.data-an].

[30] **ALICE** Collaboration, S. Acharya *et al.*, "Measurement of beauty and charm production in pp collisions at $\sqrt{s} = 5.02$ TeV via non-prompt and prompt D mesons", *JHEP* **05** (2021) 220, arXiv:2102.13601 [nucl-ex].

[31] **LHCb** Collaboration, R. Aaij *et al.*, "Measurement of J/ψ production cross-sections in *pp* collisions at $\sqrt{s} = 5$ TeV", *JHEP* **11** (2021) 181, arXiv:2109.00220 [hep-ex].

[32] **LHCb** Collaboration, R. Aaij *et al.*, "Measurement of forward J/ψ production cross-sections in pp collisions at $\sqrt{s} = 13$ TeV", *JHEP* **10** (2015) 172, `arXiv:1509.00771 [hep-ex]`. [Erratum: JHEP 05, 063 (2017)].

[33] D. J. Lange, "The EvtGen particle decay simulation package", *Nucl. Instrum. Meth. A* **462** (2001) 152–155.

[34] E. Barberio, B. van Eijk, and Z. Was, "Photos - a universal monte carlo for qed radiative corrections in decays", *Computer Physics Communications* **66** no. 1, (1991) 115–128.

[35] G. D'Agostini, "A Multidimensional unfolding method based on Bayes' theorem", *Nucl. Instrum. Meth. A* **362** (1995) 487–498.

[36] **ALICE** Collaboration, S. Acharya *et al.*, "Prompt D^0, D^+, and D^{*+} production in Pb–Pb collisions at $\sqrt{s_{NN}} = 5.02$ TeV", *JHEP* **01** (2022) 174, `arXiv:2110.09420 [nucl-ex]`.

[37] **ALICE** Collaboration, S. Acharya *et al.*, "Prompt and non-prompt J/ψ production cross sections at midrapidity in proton-proton collisions at $\sqrt{s} = 5.02$ and 13 TeV", *JHEP* **03** (2022) 190, `arXiv:2108.02523 [nucl-ex]`.

[38] **ALICE** Collaboration, S. Acharya *et al.*, "Dielectron production in proton-proton and proton-lead collisions at $\sqrt{s_{NN}} = 5.02$ TeV", *Phys. Rev. C* **102** no. 5, (2020) 055204, `arXiv:2005.11995 [nucl-ex]`.

[39] **ALICE** Collaboration, S. Acharya *et al.*, "Dielectron and heavy-quark production in inelastic and high-multiplicity proton–proton collisions at $\sqrt{s_{NN}} = 13$TeV", *Phys. Lett. B* **788** (2019) 505–518, `arXiv:1805.04407 [hep-ex]`.

[40] **ALICE** Collaboration, B. Abelev *et al.*, "Measurement of electrons from beauty hadron decays in pp collisions at $\sqrt{s} = 7$ TeV", *Phys. Lett. B* **721** (2013) 13–23, `arXiv:1208.1902 [hep-ex]`. [Erratum: Phys.Lett.B 763, 507–509 (2016)].

[41] **ALICE** Collaboration, B. B. Abelev *et al.*, "Beauty production in pp collisions at $\sqrt{s} = 2.76$ TeV measured via semi-electronic decays", *Phys. Lett. B* **738** (2014) 97–108, `arXiv:1405.4144 [nucl-ex]`. [Erratum: Phys.Lett.B 763, 507–509 (2016)].

[42] **CDF** Collaboration, D. Acosta *et al.*, "Measurement of the J/ψ meson and $b-$hadron production cross sections in $p\bar{p}$ collisions at $\sqrt{s} = 1960$ GeV", *Phys. Rev. D* **71** (2005) 032001, `arXiv:hep-ex/0412071`.

[43] **ALICE** Collaboration, S. Acharya *et al.*, "Dielectron production in proton-proton collisions at $\sqrt{s} = 7$ TeV", *JHEP* **09** (2018) 064, `arXiv:1805.04391 [hep-ex]`.

[44] L. Apolinário, Y.-J. Lee, and M. Winn, "Heavy quarks and jets as probes of the QGP", *Prog. Part. Nucl. Phys.* **127** (2022) 103990, `arXiv:2203.16352 [hep-ph]`.

[45] B. Wu, Z. Tang, M. He, and R. Rapp, "Recombination of Bc mesons in ultrarelativistic heavy-ion collisions", *Phys. Rev. C* **109** no. 1, (2024) 014906, `arXiv:2302.11511 [nucl-th]`.